Supplement of The Cryosphere, 20, 1635–1654, 2026
https://doi.org/10.5194/tc-20-1635-2026-supplement

The Cryosphere Open Access EGU

Supplement of

In situ monitoring of seasonally frozen ground using soil freezing characteristic curve in permittivity–temperature space

Hesam Salmabadi et al.

Correspondence to: Hesam Salmabadi (hesam.salmabadi@uqtr.ca)

S1 Extended Context on Soil Freezing Theory and Measurement

The Soil Freezing Characteristic Curve (SFCC), which defines the relationship between liquid water content (θ_{lw}) and subzero temperatures (Spaans and Baker, 1996; Koopmans and Miller, 1966), provides a physically-based framework for capturing the complexities of soil freezing processes (Pardo Lara et al., 2020). As illustrated in Fig. **??**, a typical SFCC is characterized by three distinct physical regimes (Zhang et al., 2019). The first, termed the "unfrozen zone," occurs when the soil temperature is above the freezing point. In this regime, the liquid water content is independent of the soil temperature; while θ_{lw} may fluctuate due to external meteorological forcing, such as precipitation or evapotranspiration, it is not governed by thermal phase change. This regime is followed by the "transitional zone," which begins immediately after the freezing point (T_f). In this zone, a sharp decrease in liquid water content occurs as the soil–water system reaches a thermodynamic balance between θ_{lw} and ice. Finally, the SFCC enters the "residual zone" at the temperature (T_{res}) where θ_{lw} stabilizes (Kozlowski, 2007; Chen et al., 2021). At this stage, bulk and capillary water have largely frozen, and the remaining liquid exists as a thin film of unfreezable or bound water held against soil particles.

The presence and behavior of θ_{lw}, and consequently the shape of the SFCC, are influenced by numerous interrelated factors, including soil mineral composition, particle size, plasticity, initial water content, dry density, solute concentration, freezing rate, confining stress, and freeze-thaw history (Chai et al., 2018; Bi et al., 2023a, b, and references therein). The T_f decreases as initial water content decreases. For example, Zhang et al. (2019) found that decreasing soil water content from 37.60% to 14.52% lowered T_f from -0.06°C to -0.75°C. Soil texture also influences the SFCC. Fine-grained soils show greater freezing point depression and gradual changes in θ_{lw}, while coarse-grained soils exhibit rapid water loss during freezing (Tian et al., 2014; Zhang et al., 2019; Bi et al., 2023b). Additionally, the freezing rate, by altering pore ice formation dynamics, solute distribution, and ice grain size, can affect both the slope and curvature of the SFCC (Watanabe and Osada, 2017). To construct the SFCC, measurements of θ_{lw} and soil temperature are required. While measuring soil temperature is relatively straightforward, accurately quantifying the θ_{lw} in frozen soil poses significant challenges, especially under field conditions.

The hysteresis between SFCC and STCC has been widely documented, particularly under laboratory conditions (Wu et al., 2017; Mavrovic et al., 2020; Pardo Lara et al., 2020). In situ studies, such as Tomaškovičová and Ingeman-Nielsen (2024), reported approximately 10% higher unfrozen water content during freezing than during thawing at equivalent temperatures within the active layer of saturated, fine-grained permafrost-affected soils, reflecting latent heat effects, cryosuction, and slow pore-water redistribution. Similarly, Overduin et al. (2006) documented asymmetric freezing–thawing transitions in saturated silty clays caused by latent heat and moisture migration. By contrast, near-surface, non-permafrost measurements found hysteresis to be theoretically expected but generally weak or indistinguishable (Pardo Lara et al., 2020).

S2 Extended Context on Technical Challenges in Estimating Unfrozen Water Content from Dielectric Measurements

Typically, both physically based models, such as dielectric mixing models, and empirical models are employed to relate ε_{eff} to θ_{uw} when using dielectric probes. To apply dielectric mixing models, the ice component must be incorporated into the model (Amankwah et al., 2022). However, solving these models is not feasible without accurate knowledge of the ice content, a challenging parameter to measure, particularly in situ, where the total water content is often unknown and uncontrollable (He and Dyck, 2013). As demonstrated by Amankwah et al. (2022), without prior knowledge of the total water content before freezing, dielectric measurements can only provide a range for the unfrozen water content rather than the exact value. Neglecting the ice component in dielectric mixing models introduces significant uncertainty and leads to overestimation of θ_{uw} (Zhou et al., 2014). This overestimation occurs because frozen soils, at identical liquid water contents, exhibit a higher ε_{eff} than drying soils, due to the higher ε_r of ice (≈ 3.2) compared to air (≈ 1). Consequently, calibrations from unfrozen soils results in systematic overprediction of θ_{uw} in frozen soils, as the increased ε_{eff} is incorrectly attributed to additional liquid water rather than the presence of ice (Spaans and Baker, 1995). Empirical models also face limitations. Most calibration equations are developed for unfrozen soils under thawed conditions (Yoshikawa and Overduin, 2005), rendering them inapplicable to frozen soils (He and Dyck, 2013). Calibration equations specifically developed for frozen soils are often limited to saturated soils (Michael W Smith and Tice, 1988) or specific soil types that require knowledge of the soil's total water content prior to freezing (Spaans and Baker, 1995). As Spaans and Baker (1995) demonstrated, a single, universal calibration equation for

measuring unfrozen water content in frozen soils using dielectric probes is unattainable. Given these challenges, constructing the SFCC based on measurements of θ_{uw} is problematic, especially in dynamic field environments.

S3 Modeled Soil Data

Soil physical property data were obtained from Geng et al. (2025). A summary of these properties at the network level is presented in Table S1, while site-specific data for each monitoring station are available at https://hesam-salmabadi.github.io/Soil-Temperature-Permittivity-Monitoring-Sites/.

Table S1. Modeled soil physical properties and organic carbon across networks.

Network Name	Count	Sand (%)	Clay (%)	Silt (%)	SOC	BD (g/cm^3)
James Bay (BJ)	14	87.7%	1.4%	10.9%	0.74	1.32
Candle Lake (BT)	17	83.3%	4.2%	12.5%	2.91	1.06
La Romaine (LR)	3	70.0%	3.9%	26.2%	1.57	1.19
Montmorency Forest (FM)	29	60.0%	11.2%	28.8%	4.66	1.13
George River (GR)	1	60.2%	7.8%	32.0%	5.40	1.15
Chapleau (CP)	4	46.7%	8.4%	45.0%	2.25	1.26
Kenaston (KN)	37	36.4%	27.6%	36.0%	3.17	1.16
Trail Valley Creek (TV)	12	31.2%	22.2%	46.5%	3.02	1.17

S4 Extended SFCC Parameter Data

Table S2 summarizes the average initial volumetric water content (VWC) at the network level (values converted from initial permittivity measurements using manufacturer-specific calibrations). The table also provides the arithmetic means for the b and T_f parameters across each network, along with the total number of recorded freezing cycles analyzed for each network.

Table S2. Soil Freezing Characteristic Curve (SFCC) parameters by network.

Network	Cycle Count	Avg. b-parameter	Avg. T_f (°C)	Avg. initial VWC (m^3/m^3)
Kenaston (KN)	70	1.05	0.16	0.278
George River (GR)	1	4.85	0.35	0.393
Montmorency (FM)	3	3.96	0.38	0.258
Trail Valley (TV)	7	3.03	0.14	0.239
James Bay (BJ)	2	2.63	0.61	0.220
Chapleau (CP)	3	3.47	0.42	0.199
La Romaine (LR)	1	4.25	0.44	0.122
Candle Lake (BT)	9	1.51	0.24	0.076

S5 Biome-Level Parameter Estimation

Site-level land cover information was obtained from the MODIS/Terra+Aqua Land Cover Type Yearly L3 Global 500m SIN Grid (V061), utilizing the University of Maryland (UMD) classification scheme for this analysis (Friedl and Sulla-Menashe, 2022). In addition to the network-level analysis, we performed hierarchical partial pooling at the biome level to further account for regional variability. The resulting b and T_f values from this analysis are presented in Tables S3 and S4 for additional reference.

Table S3. Biome-level b parameters with 95% Highest Density Intervals (HDI).

Biome	Mean	HDI 2.5%	HDI 97.5%
Croplands	1.000	0.480	1.574
Evergreen Needleleaf Forests	1.572	0.254	3.554
Mixed Forests	3.149	1.324	5.193
Open Shrublands	2.863	1.288	4.531
Savannas	2.230	0.703	4.020
Woody Savannas	1.675	0.832	2.671

Table S4. Biome-level T_f (°C) parameters with 95% Highest Density Intervals (HDI).

Biome	Mean	HDI 2.5%	HDI 97.5%
Croplands	0.139	−0.159	0.419
Evergreen Needleleaf Forests	0.004	−0.788	0.794
Mixed Forests	0.327	0.002	0.648
Open Shrublands	0.151	−0.177	0.445
Savannas	0.395	−0.079	0.883
Woody Savannas	0.230	−0.084	0.537

S6 Supplementary Figures

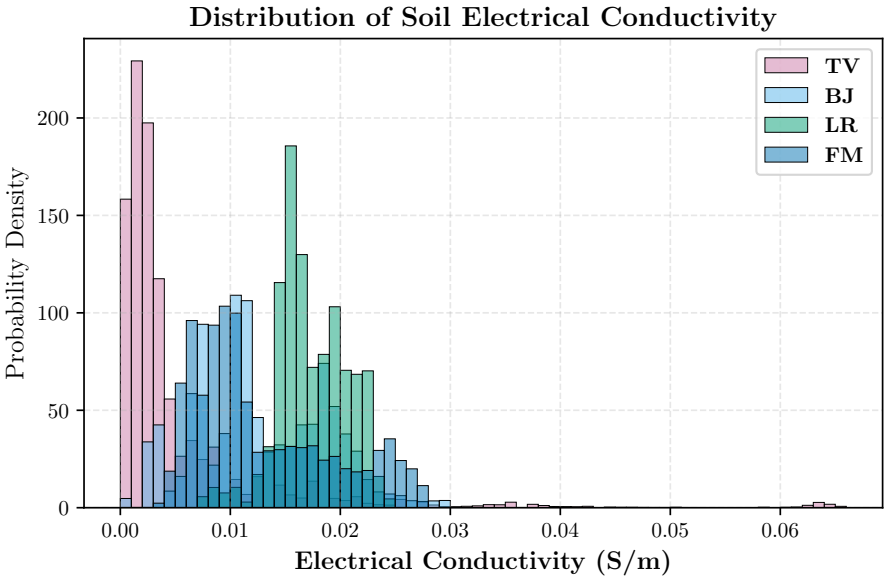

Figure S1. Histogram of electrical conductivity (EC) values measured at Trail Valley Creek (TV), James Bay (BJ), La Romaine (LR), and Montmorency Forest (FM) sites.

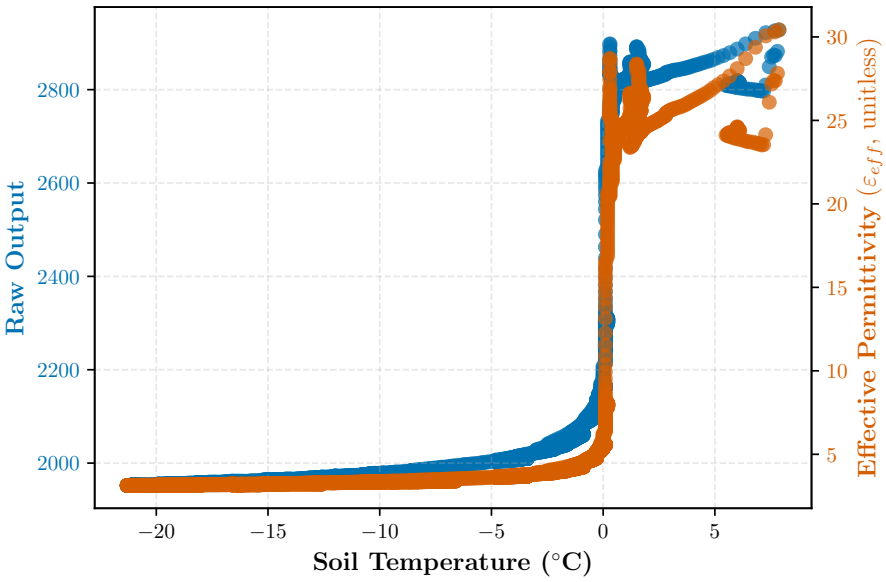

Figure S2. Soil Freezing Characteristic Curve (SFCC) visualized in both sensor raw output–temperature space and permittivity–temperature space. These representations highlight the freezing transition as captured directly by the sensor output and after conversion to effective permittivity.

References

Amankwah, S. K., Ireson, A. M., and Brannen, R.: An improved model and field calibration technique for measuring liquid water content in unfrozen and frozen soils with dielectric probes, Vadose Zone Journal, 21, e20 225, https://doi.org/10.1002/vzj2.20225, 2022.

Bi, J., Wang, G., Wu, Z., Wen, H., Zhang, Y., Lin, G., and Sun, T.: Investigation on unfrozen water content models of freezing soils, Frontiers in Earth Science, 10, 1039 330, https://doi.org/10.3389/feart.2022.1039330, 2023a.

Bi, J., Wu, Z., Lu, Y., Wen, H., Zhang, Y., Shen, Y., Wei, T., and Wang, G.: Study on soil freezing characteristic curve during a freezing-thawing process, Frontiers in Earth Science, 10, 1007 342, https://doi.org/10.3389/feart.2022.1007342, 2023b.

Chai, M., Zhang, J., Zhang, H., Mu, Y., Sun, G., and Yin, Z.: A method for calculating unfrozen water content of silty clay with consideration of freezing point, Applied Clay Science, 161, 474–481, https://doi.org/10.1016/j.clay.2018.05.015, 2018.

Chen, Y., Zhou, Z., Wang, J., Zhao, Y., and Dou, Z.: Quantification and division of unfrozen water content during the freezing process and the influence of soil properties by low-field nuclear magnetic resonance, Journal of Hydrology, 602, 126 719, https://doi.org/10.1016/j.jhydrol.2021.126719, 2021.

Friedl, M. and Sulla-Menashe, D.: MODIS/Terra+Aqua Land Cover Type Yearly L3 Global 500m SIN Grid V061, https://doi.org/10.5067/MODIS/MCD12Q1.061, 2022.

Geng, X., He, J., Grima, V., Jiang, Y., Tetreau, M., Crittenden, S., Kiley, S., VandenBygaart, A. J., and Vanrobaeys, J.: 100 m soil landscape grids of Canada, Scientific Data, 12, 1178, https://doi.org/10.1038/s41597-025-05460-4, 2025.

He, H. and Dyck, M.: Application of Multiphase Dielectric Mixing Models for Understanding the Effective Dielectric Permittivity of Frozen Soils, Vadose Zone Journal, 12, vzj2012.0060, https://doi.org/10.2136/vzj2012.0060, _eprint: https://onlinelibrary.wiley.com/doi/pdf/10.2136/vzj2012.0060, 2013.

Koopmans, R. W. R. and Miller, R. D.: Soil Freezing and Soil Water Characteristic Curves, Soil Science Society of America Journal, 30, 680–685, https://doi.org/10.2136/sssaj1966.03615995003000060011x, 1966.

Kozlowski, T.: A semi-empirical model for phase composition of water in clay–water systems, Cold Regions Science and Technology, 49, 226–236, https://doi.org/10.1016/j.coldregions.2007.03.013, 2007.

Mavrovic, A., Pardo Lara, R., Berg, A., Demontoux, F., Royer, A., and Roy, A.: Soil dielectric characterization at L-band microwave frequencies during freeze-thaw transitions, https://doi.org/10.5194/hess-2020-291, 2020.

Michael W Smith and Tice, A. R.: Measurement of the Unfrozen Water Content of Soils. Comparison of NMR (Nuclear Magnetic Resonance) and TDR (Time Domain Reflectometry) Methods, CRREL Rep. 88-18. U.S. Army Corps of Engineers, Cold Regions Research and Engineering Lab, Hannover, NH., https://apps.dtic.mil/sti/tr/pdf/ADA203082.pdf, accessed: 2024-09-20, 1988.

Overduin, P., Kane, D., and Van Loon, W.: Measuring thermal conductivity in freezing and thawing soil using the soil temperature response to heating, Cold Regions Science and Technology, 45, 8–22, https://doi.org/10.1016/j.coldregions.2005.12.003, 2006.

Pardo Lara, R., Berg, A. A., Warland, J., and Tetlock, E.: In Situ Estimates of Freezing/Melting Point Depression in Agricultural Soils Using Permittivity and Temperature Measurements, Water Resources Research, 56, e2019WR026 020, https://doi.org/10.1029/2019WR026020, _eprint: https://onlinelibrary.wiley.com/doi/pdf/10.1029/2019WR026020, 2020.

Spaans, E. J. A. and Baker, J. M.: Examining the use of time domain reflectometry for measuring liquid water content in frozen soil, Water Resources Research, 31, 2917–2925, https://doi.org/10.1029/95WR02769, 1995.

Spaans, E. J. A. and Baker, J. M.: The Soil Freezing Characteristic: Its Measurement and Similarity to the Soil Moisture Characteristic, Soil Science Society of America Journal, 60, 13–19, https://doi.org/10.2136/sssaj1996.03615995006000010005x, 1996.

Tian, H., Wei, C., Wei, H., and Zhou, J.: Freezing and thawing characteristics of frozen soils: Bound water content and hysteresis phenomenon, Cold Regions Science and Technology, 103, 74–81, https://doi.org/10.1016/j.coldregions.2014.03.007, 2014.

Tomaškovičová, S. and Ingeman-Nielsen, T.: Quantification of freeze–thaw hysteresis of unfrozen water content and electrical resistivity from time lapse measurements in the active layer and permafrost, Permafrost and Periglacial Processes, 35, 79–97, https://doi.org/10.1002/ppp.2201, 2024.

Watanabe, K. and Osada, Y.: Simultaneous measurement of unfrozen water content and hydraulic conductivity of partially frozen soil near 0 °C, Cold Regions Science and Technology, 142, 79–84, https://doi.org/10.1016/j.coldregions.2017.08.002, 2017.

Wu, Y., Nakagawa, S., Kneafsey, T. J., Dafflon, B., and Hubbard, S.: Electrical and seismic response of saline permafrost soil during freeze - Thaw transition, Journal of Applied Geophysics, 146, 16–26, https://doi.org/10.1016/j.jappgeo.2017.08.008, 2017.

Yoshikawa, K. and Overduin, P. P.: Comparing unfrozen water content measurements of frozen soil using recently developed commercial sensors, Cold Regions Science and Technology, 42, 250–256, https://doi.org/10.1016/j.coldregions.2005.03.001, 2005.

Zhang, M., Zhang, X., Lu, J., Pei, W., and Wang, C.: Analysis of volumetric unfrozen water contents in freezing soils, Experimental Heat Transfer, 32, 426–438, https://doi.org/10.1080/08916152.2018.1535528, 2019.

Zhou, X., Zhou, J., Kinzelbach, W., and Stauffer, F.: Simultaneous measurement of unfrozen water content and ice content in frozen soil using gamma ray attenuation and TDR, Water Resources Research, 50, 9630–9655, https://doi.org/10.1002/2014WR015640, 2014.